

Transition from reversible to irreversible flow: Absorbing and depinning transitions in a sheared-vortex system

S. Okuma, Y. Tsugawa, and A. Motohashi

Research Center for Low Temperature Physics, Tokyo Institute of Technology, 2-12-1, Ohokayama, Meguro-ku, Tokyo 152-8551, Japan

(Received 20 November 2010; published 10 January 2011)

We provide evidence that a reversible to irreversible flow transition (RIT), as reported in driven colloidal particles, occurs in periodically sheared vortices in a Corbino-disk superconductor under increasing a displacement d of vortices per cycle. We determine a threshold displacement d_c for RIT as the onset of flow noise. A relaxation time to reach the steady state diverges around d_c , indicative of an absorbing transition from self-organized nonfluctuating (reversible) to fluctuating diffusing (irreversible) states. Our results strongly suggest that RIT is a universal phenomenon in driven interacting particle systems with quenched disorder. We also find evidence for a depinning transition with critical behavior similar to that of the absorbing transition in the same vortex system.

DOI: [10.1103/PhysRevB.83.012503](https://doi.org/10.1103/PhysRevB.83.012503)

PACS number(s): 74.25.Uv, 74.40.-n, 05.70.Ln, 62.20.F-

In many-particle systems where their dynamics is dominated by time-reversible equations of motion, irreversible phenomena are often visible. In slowly sheared colloidal particles placed between concentric cylinders, a novel dynamic transition from reversible to irreversible flow has been observed.^{1,2} In a reversible regime, the colloids return to their initial position at the end of each cycle of a periodic shear, while in an irreversible regime, they do not return to their initial position. Both regimes are identified by a displacement of colloids per cycle and its threshold has been determined. This transition, called reversible to irreversible transition (RIT), is expected to occur widely in nature but not yet verified experimentally. Understanding of the phenomenon will lead to new insights into the relationship between chaos, reversibility, and predictability,¹ which is a fundamental issue in statistical physics. In an effort to clarify the universality of the phenomenon, it has been shown numerically^{3,4} that periodically driven superconducting vortices exhibit a similar transition under increasing cycle period (displacement d) and that it can be readily detected by the onset of broadband voltage noise (BBN) S_V .³

Recently, Corté *et al.* have carried out further numerical and experimental studies for the colloidal system.⁵ They suddenly applied a periodic shear and examined a transient behavior. The particles collide with each other feeling a random force and hence the system starts in a fluctuating state. After a certain relaxation time, the system organizes into either a fluctuating steady state or a nonfluctuating single quiescent state. The latter state is interpreted as an absorbing state, from which a system can never escape.^{3,5-11} Since the irreversible collisions that generally produce diffusive chaotic dynamics can also cause a system to self-organize to avoid future collisions, this is termed random organization.⁵ Interestingly, the relaxation time diverges at the shearing threshold (RIT), which is identified with an absorbing transition. The concept of self-organization is important in explaining origins of order, e.g., in biological and social systems, and in controlling the structure of materials microscopically.⁵ It is of great interest to explore whether reversible to irreversible behaviors and random organization found in the colloidal system can be generalized to other nonequilibrium many-body systems.^{3,4,12}

Here, we conduct shearing experiments for vortices confined in a Corbino disk (CD) of an amorphous (a -)Mo_xGe_{1-x} film with random point pinning. In the presence of a radial current I , the vortices rotate around the center of CD by feeling a frustrated Lorentz force inversely proportional to the radius r of rotation.^{13,14} We have driven the vortices periodically in the circumferential direction by applying an ac square current I_{ac} , which, together with pinning, gives rise to a shearing motion for vortices relative to each other, and measured S_V as a function of displacement d per half a cycle. We observe the field(B)-dependent threshold d_c above which S_V appears: d_c is large when the vortex solid is rigid and uniform, consistent with the picture of RIT. We have also measured the time (t) evolution of voltage $V(t)$ just after I_{ac} was applied. The amplitude of $V(t)$ shows an increase with t , relaxing toward a steady-state value. The relaxation time $\tau_1(d)$ diverges around d_c , providing a strong support for RIT and absorbing transition at d_c . We also find evidence for the depinning transition,^{6,15} which falls into the class of the absorbing transition. Preliminary results have been reported elsewhere.¹⁶

The 330-nm-thick a -Mo_xGe_{1-x} film was prepared by rf sputtering on a Si substrate held at room temperature.¹⁷ Mean-field transition and zero-resistivity temperatures are 6.3 and 6.2 K, respectively. Arrangement of silver electrical contacts is shown schematically in the inset (left bottom) of Fig. 1(a). The current flows between the contact $+C$ of the center and that $-C$ of the perimeter of the disk, which produces a radial current density that decays as $1/r$. The inner radius of CD is 0.8 mm. We used the voltage contacts, $+V$ and $-V$, to measure the voltage V and voltage noise S_V . In measuring noise spectra, voltage enhanced with a preamplifier was analyzed with a fast-Fourier transform spectrum analyzer. We obtained excess noise spectra by subtracting the background contribution, which was measured with $I = 0$. The field B was applied perpendicular to the plane of the film.

All the data were taken at 4.1 K for different B corresponding to the solid phase.¹⁷ As illustrated with gray dots in the inset (left top) of Fig. 1(a), we applied I_{ac} of square wave form, whose amplitude was fixed to yield ac voltage with constant amplitude V^∞ ($\approx 10 \mu\text{V}$) in the steady state. For

10 μV the flow state is pinning-dominated plastic flow. The period t_{ac} of I_{ac} was varied from 0.125 to 25 ms to change d in the range $\approx 0.5\text{--}10^2 \mu\text{m}$. Here, d is calculated from the relation $d = V^\infty t_{ac}/2Bl$, where l is a distance between voltage contacts. The right inset shows the selected data of noise spectra taken for different d (t_{ac}) in 3.2 T, which is just below the peak field B_p ($=3.25 \text{ T}$) of the depinning current $I_d(B)$ shown in Fig. 2(b). The field of B_p marks the structural transition of vortex matter from the ordered phase (OP) to amorphouslike disordered phase (DP).¹⁷ This order-disorder transition¹⁸ is evidenced from a sharp maximum and subsequent abrupt drop of $S_V(B)$ at B_p , as indicated with full circles in Fig. 2(b). Large $S_V(B)$ observed just below B_p implies the coexistence of OP and DP, where vortex flow is most disordered.¹⁷

Spectral shape of S_V is of Lorentzian type, while many spikes or narrow-band noise originating from the fundamental ($1/t_{ac}$) and higher order frequencies of I_{ac} are visible superimposed on BBN. Some of them are eliminated from the figure for clarity. For small d , e.g., $d = 1.30 \mu\text{m}$, some data points are missing from the spectra, indicating that S_V is close to or below the background level ($\sim 10^{-18} \text{ V}^2/\text{Hz}$), while for larger d substantial BBN exceeding the background level appears. In Fig. 1(a) we plot the d dependence of S_V at low frequency (100 Hz) in 3.2 T. For d smaller than about $2 \mu\text{m}$, $S_V(100 \text{ Hz})$ (open circles) is below the background level (shading). As d exceeds about $2 \mu\text{m}$, $S_V(100 \text{ Hz})$ (full circles) starts to rise and increases almost linearly with d . Qualitatively the same result is obtained for other B studied.

The simulations³ consider vortex dynamics in a square-shaped superconductor with periodic boundary conditions, that is, no sample edges. In our experiment the absence of sample edges is a necessary condition to eliminate complicated edge effects¹⁸ and to compare our results with those of the colloidal system. This condition is certainly satisfied by using CD,^{13,14} while large shear forces that are actually present both in CD^{13,14} and colloids are not considered in the simulations. We will show, however, that qualitative features of RIT observed in our work are consistent with the numerical results. The simulation³ determined stroboscopically the location of vortices driven by periodic drive and calculated the mean square vortex displacement, equivalently, effective diffusivity D . In the reversible regime D is zero, while in the irreversible regime $D > 0$. It is also shown that there is an initial transient period for finite D [$> D(t \rightarrow \infty)$], after which the system settles into the stationary state that is either reversible [$D(t \rightarrow \infty) = 0$] or irreversible [$D(t \rightarrow \infty) > 0$].

Here, we begin by considering the behavior after the stationary state is reached. The D vs d curve reported in Ref. 3 is qualitatively similar to the S_V vs d curve shown in Fig. 1(a), although the relationship between D and S_V is unclear. The critical value d_c is determined from the simple linear extrapolation of the data (full circles) to the abscissa ($S_V = 0$); e.g., $d_c \approx 1.6$ [an arrow in Fig. 1(a)] and $4 \mu\text{m}$ (not shown here), which correspond to the angles of 0.2° and 0.5° around the center of CD, for 3.2 and 1 T, respectively. We interpret d_c as the threshold displacement of RIT. In the field region ($\sim 1 \text{ T}$) studied an intervortex spacing a_0 is around 10 nm, which is well below the London penetration depth ($\sim 1 \mu\text{m}$), and $d_c \sim 1 \mu\text{m}$ corresponds to a

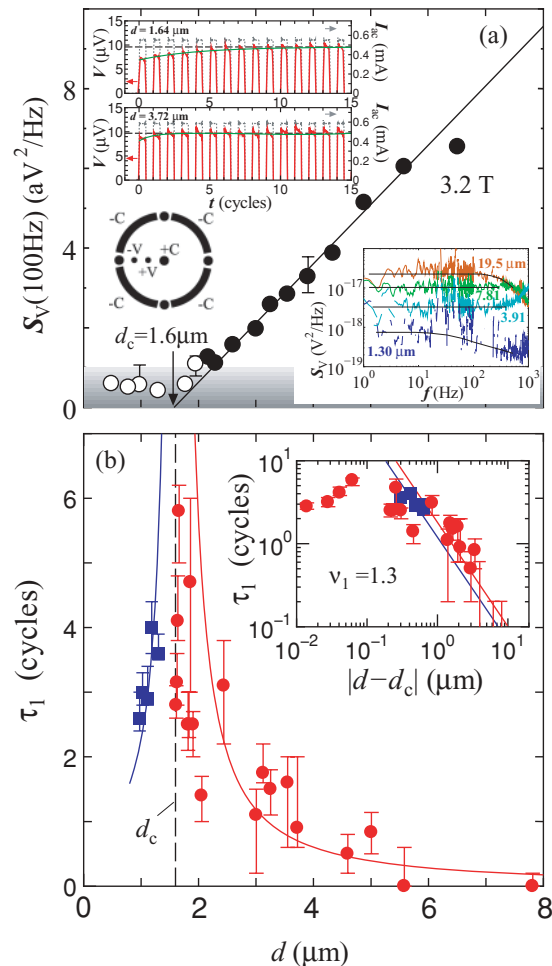


FIG. 1. (Color online) (a) $S_V(100 \text{ Hz})$ in 3.2 T vs d . Open circles denote $S_V(100 \text{ Hz})$ below the background level and an arrow marks d_c . Inset: (Left top) Gray dots and a horizontal dashed line represent I_{ac} and amplitude of ac voltage in the steady state, respectively. Red (dark gray) lines indicate $V(t)$ in 3.2 T for $d = 1.64$ and $3.72 \mu\text{m}$ vs number of shear cycles. (Left bottom) Arrangement of the electrical contacts. (Right) Noise spectra for different d in 3.2 T. Lines are guide to the eye. (b) τ_1 vs d . Squares and circles represent the data below and above d_c (a vertical dashed line), respectively, at which τ_1 diverges. Full lines on both sides of the threshold show power-law fits. Inset: The same data and its fits plotted on a log-log scale.

distance ($\sim 10^2 \times a_0$) over which a few hundred vortices are located.

Next, we focus on the transient behavior, which was measured at 3.2 T in the disordered flow regime just below B_p . The inset (left top) of Fig. 1(a) shows the time evolution of $V(t)$ vs the number of shear cycles taken for $d = 1.64 \mu\text{m}$ just above d_c ($=1.6 \mu\text{m}$) and $3.72 \mu\text{m}$. Since the voltage is proportional to the average vortex velocity, a transient motion of vortices can be sensitively detected by $V(t)$. To randomize the initial vortex distribution, for each measurement we first shear the system at a large displacement by applying I_{ac} with $t_{ac} = 20 \text{ ms}$ ($d = 80 \mu\text{m}$) for more than 20 s (10^3 cycles). For $d = 1.64 \mu\text{m}$ the amplitude of voltage $|V(t)|$ ($\equiv V^0$) at $t = 0$ is smaller than that of $|V(t)|$ ($\equiv V^\infty$) at $t \rightarrow \infty$ or the dc voltage (10 μV). This is because initial vortex distributions are random

and the first several cycles generate many collisions, similarly to the case of colloids. After the several cycles, $|V(t)|$ increases and eventually reaches the steady-state value $V^\infty \approx 10 \mu\text{V}$. Essentially the same vortex dynamics in response to ac drive was reported earlier in NbSe₂.¹⁹ For larger $d = 3.72 \mu\text{m}$ ($\approx 2d_c$) a transient behavior of $V(t)$ is also observed, but it is much less pronounced. For $d < d_c$, we observe almost the same transient behavior (not shown here) as that for $d > d_c$. However, the situation is much different depending on whether d is smaller or larger than d_c .⁵ For $d < d_c$, which corresponds to the reversible state, all the vortices eventually find a position such that they no longer collide with each other when the system is sheared. By contrast, for $d > d_c$, which corresponds to the irreversible state, the system reaches the steady state where nonzero fraction of vortices always collides with another vortex.

To verify the validity of the above interpretation and get more insights into random organization,^{5,6} we examine the characteristic time τ ($\equiv \tau_1$) for the system to reach the steady state. τ_1 is extracted by fitting $|V(t)|$ to the simple relaxation function,^{5,6}

$$|V(t)| = V^\infty - (V^\infty - V^0) \exp(-t/\tau)/t^\alpha. \quad (1)$$

Here, we fix α ($\equiv \alpha_1$) to be zero, because theoretically the value of α_1 only becomes relevant very close to the transition ($\tau_1 \rightarrow \infty$), while in our experiment τ_1/t is relatively small. In Fig. 1(b) we plot τ_1 against d . For $d < 1 \mu\text{m}$, we cannot obtain reliable data because of limitation of fast $V(t)$ measurements. The divergence in τ_1 is visible around $1.6 \mu\text{m}$ ($\approx d_c$), which strongly supports the view that the absorbing transition from nonfluctuating (reversible) to fluctuating (irreversible) states occurs at d_c and that d_c obtained from S_V indeed probes RIT. The τ_1 vs d curves on both sides of the transition can be fit to a power-law form, $\tau_1 \propto |d - d_c|^{-\nu_1}$ with $\nu_1 = 1.3$, as shown with full lines. The inset displays the same data plotted on a log-log scale, giving $\nu_1 = 1.3 \pm 0.3$. Our exponent is close to 1.1 ± 0.3 and 1.33 ± 0.02 reported in the colloidal experiments and simulations, respectively.^{5,6}

The simulations predict that the reversible to irreversible behaviors are largely dependent on the vortex-vortex interaction (B)³ and driving force.⁴ In particular, in the peak effect regime just prior to B_p , where the effectiveness of pinning changes sharply with B , it should be possible to observe RIT only by changing B at fixed d . This is seen in Fig. 2(a), where d_c derived from S_V is plotted against B . Also shown between Figs. 2(a) and 2(b) is the equilibrium vortex phase diagram constructed based on B dependences of I_d and flow noise (S_V at 100 Hz divided by V)¹⁷ [Fig. 2(b)]. We find that d_c is zero, namely, reversibility is completely lost both for low B (< 0.5 T) in OP and for high B in DP, i.e., just below the melting field B_c and in the liquid phase. In these particular B regions the vortex solids are softer than in the intermediate B region (1–2.3 T) within OP, which accounts for the suppression of the reversible behavior. Quite recently, we have detected softening of rotating vortex lattices at low B by a mode-locking experiment for the same CD sample as a change in lattice orientation with respect to the flow direction.¹⁴ It is also noted in Fig. 2(a) that as the field is increased from $B = 0$ at fixed d , the irreversible-to-reversible behavior occurs at certain

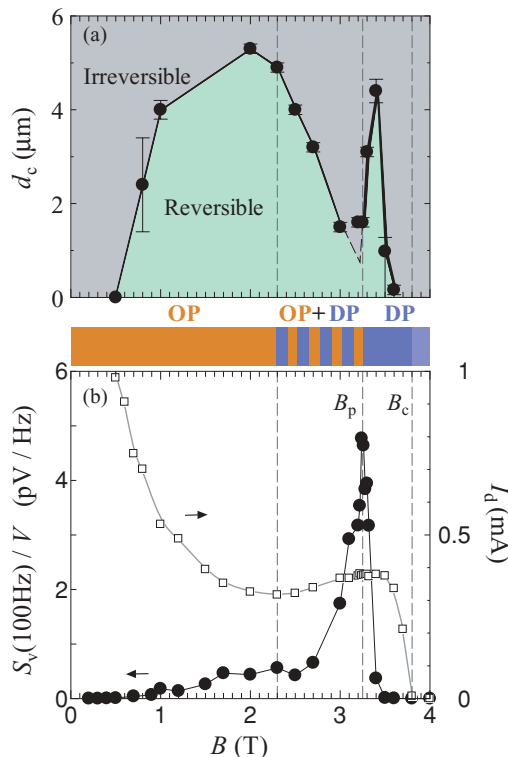


FIG. 2. (Color online) (a) d_c vs B . (b) $S_V(100 \text{ Hz}) / V$ (full circles) and depinning I_d (open squares) as a function of B . Static vortex phase diagram is illustrated between (a) and (b). Vertical dashed lines mark the onset of the coexistence phase in OP (left), ODT (B_p) (middle), and melting B_c (right). Other lines are guide to the eye.

$B(d)$, consistent with numerical work predicting qualitatively the same behavior when one enters a jammed phase.³ While the simulation has not made specific predictions at higher B including the peak effect regime, our results clearly show that reversibility (d_c) is sharply suppressed in fields just prior to B_p . This behavior is reasonable, considering that vortex flow is most disordered in the coexistence phase.¹⁷ The peculiar field dependence of d_c shown in Fig. 2(a), which well reflects the static vortex states (rigidity and uniformity), can be a further support for RIT at d_c .

Finally, we discuss plastic depinning¹⁵ based on $V(t)$ just after dc I is suddenly applied. The transient vortex motion based on $V(t)$ was studied earlier for NbSe₂.¹⁹ In plastic depinning for two dimensions (2D), particles move in the form of complex fluctuating channels, where some particles are mobile while others remain pinned. This phenomenon is widespread in nature,¹⁵ but the true nature of the depinning transition is still not fully understood. Quite recently, similarity between random organization (absorbing transition) and plastic depinning (depinning transition) has been proposed numerically.⁶ The simulation predicts that the system exhibits a transient behavior before settling into a completely pinned state or a steady moving state, depending on whether the driving force is below ($I < I_d$) or above ($I > I_d$) the threshold pinning force, respectively.

We measure $V(t)$ in 3.0 T, where pinning is so effective. Before applying I , the field was decreased and then increased

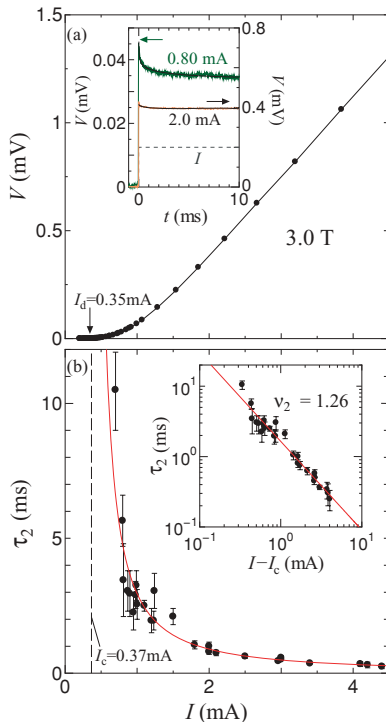


FIG. 3. (Color online) (a) $I - V$ relation in 3.0 T. An arrow marks I_d . Inset: $V(t)$ just after dc I (0.8, 2.0 mA) was applied. Full lines are fits to Eq. (1). A dashed line illustrates the shape of $I(t)$. (b) τ_2 vs I , exhibiting a divergence at $I_c = 0.37 \pm 0.15$ mA (a vertical dashed line) close to $I_d \approx 0.35$ mA. A red (dark gray) line shows a power law fit. Inset: The same data and its fit on a log-log scale.

up to 3.0 T. This field sweep process is necessary to avoid a situation that many vortices are strongly pinned in the initial state. For $I < I_d$ detectable $V(t)$ is not visible, while above I_d we observe decaying $V(t)$. Here, I_d (≈ 0.35 mA) is determined

from $I - V$ relation in Fig. 3(a). In the inset we display the typical decaying signals of $V(t)$ for $I = 0.8$ and 2.0 mA, which are slightly and well above I_d , respectively. The decay time τ_2 for 0.8 mA looks longer than for 2.0 mA. We can reproduce the $V(t)$ curves well above I_d using a simple exponential function, while in the vicinity of I_d the functional form approaches a power law. Thus, to obtain τ_2 , we fit $V(t)$ to the same function as Eq. (1). Near I_d , $\alpha_2 (\equiv \alpha_2) \approx 0.4$. As shown in Fig. 3(b), $\tau_2(I)$ diverges at $0.37(\pm 0.15) (\equiv I_c)$ mA that is close to $I_d \approx 0.35$ mA and the data points fall onto a line expressed as $\tau_2 \propto (I - I_c)^{-\nu_2}$ with $\nu_2 \approx 1.26$. The same data are plotted on a log-log scale in the inset, giving $\nu_2 = 1.26 \pm 0.15$. Our exponent ν_2 , as well as $\alpha_2 \approx 0.4$ near I_c , is close to $\nu_2 = 1.36 \pm 0.06$ ($\alpha_2 = 0.5$) reported in simulation for the depinning transition in 2D⁶ and also close to $\nu_1 = 1.1 \pm 0.3$ and 1.33 ± 0.02 found in the colloidal experiment in 3D and simulation for random organization in 2D,⁵ respectively. We thus conclude that the nonequilibrium absorbing and depinning transitions actually occur in our 2D vortex system and exhibit the similar critical behavior, indicating that both transitions fall into the same universal class.⁶

It is of interest to elucidate microscopic mechanisms giving rise to plastic depinning and irreversible flow²⁰: RIT may be interpreted as a “plastic depinning transition” where irreversible vortex motion occurs in correspondence with flow of topological defects in lattice. Quenched disorder favors these defects and the transition is accompanied by the onset of BBN. For CD, a simulation showed that BBN appears accompanying the dynamics of topological defects even in the absence of quenched disorder.²¹ This work will stimulate further research into a connection between the onset of irreversibility and dislocation dynamics,²⁰ as well as the relationship between chaos, self-organization, and reversibility.¹

We thank C. Reichardt for helpful discussions.

¹D. J. Pine, J. P. Gollub, J. F. Brady, and A. M. Leshansky, *Nature (London)* **438**, 997 (2005).

²J. Gollub and D. Pine, *Phys. Today* **59**, 8 (2006).

³N. Mangan, C. Reichardt, and C. J. Olson Reichardt, *Phys. Rev. Lett.* **100**, 187002 (2008).

⁴W. Zhang, W. Zhou, and M. Luo, *Phys. Lett. A* **374**, 3666 (2010).

⁵L. Corté, P. M. Chaikin, J. P. Gollub, and D. J. Pine, *Nature Phys.* **4**, 420 (2008).

⁶C. Reichardt and C. J. Olson Reichardt, *Phys. Rev. Lett.* **103**, 168301 (2009).

⁷H. Hinrichsen, *Adv. Phys.* **49**, 815 (2000).

⁸R. Dickman, *Physica A* **306**, 90 (2002).

⁹K. A. Takeuchi, M. Kuroda, H. Chaté, and M. Sano, *Phys. Rev. Lett.* **99**, 234503 (2007).

¹⁰F. Vazquez, V. M. Eguiluz, and M. S. Miguel, *Phys. Rev. Lett.* **100**, 108702 (2008).

¹¹G. I. Menon and S. Ramaswamy, *Phys. Rev. E* **79**, 061108 (2009).

¹²D. G. Grier, *Nature (London)* **424**, 810 (2003).

¹³D. López, W. K. Kwok, H. Safar, R. J. Olsson, A. M. Petrean, L. Paulius, and G. W. Crabtree, *Phys. Rev. Lett.* **82**, 1277 (1999).

¹⁴S. Okuma, Y. Yamazaki, and N. Kokubo, *Phys. Rev. B* **80**, 220501(R) (2009): Over broad B we observe a mode locking resonance suggesting the formation of rotating vortex rings composed of triangular arrays.

¹⁵M. C. Marchetti and K. A. Dahmen, *Phys. Rev. B* **66**, 214201 (2002); M. B. Luo and X. Hu, *Phys. Rev. Lett.* **98**, 267002 (2007); A. Pertsinidis and X. S. Ling, *ibid.* **100**, 028303 (2008).

¹⁶S. Okuma, Y. Suzuki, and Y. Tsugawa, *Physica C* **470**, S842 (2010).

¹⁷S. Okuma, K. Kashiro, Y. Suzuki, and N. Kokubo, *Phys. Rev. B* **77**, 212505 (2008).

¹⁸Y. Paltiel, E. Zeldov, Y. Myasoedov, M. L. Rappaport, G. Jung, S. Bhattacharya, M. J. Higgins, Z. L. Xiao, E. Y. Andrei, P. L. Gammel, and D. J. Bishop, *Phys. Rev. Lett.* **85**, 3712 (2000).

¹⁹W. Henderson, E. Y. Andrei, and M. J. Higgins, *Phys. Rev. Lett.* **81**, 2352 (1998).

²⁰P. Moretti and M. Carmen Miguel, *Phys. Rev. B* **80**, 224513 (2009).

²¹M. C. Miguel and S. Zapperi, *Nature Mat.* **2**, 477 (2003).